J Electr Eng Technol Vol. 9, No. 6: 1914-1920, 2014
http://dx.doi.org/10.5370/JEET.2014.9.6.1914

ISSN(Print) 1975-0102
ISSN(Online) 2093-7423

Analysis on Core Loss of Brushless DC Motor Considering Pulse Width Modulation of Inverter

Ki-Chan Kim†

Abstract – In this paper, characteristics of blushless direct current (BLDC) motor including core loss are analyzed considering pulse width modulation (PWM) of inverter. Input voltage of BLDC motor due to PWM is calculated considering duty ratio and carrier frequency of inverter in order to control torque or speed of BLDC motor. For the calculation of core loss, the input current with harmonics due to PWM voltage is calculated by using equivalent circuit model of BLDC motor according to switching pattern and carrier frequency. Next, core loss is analyzed by inputting the currents as a source of BLDC motor for FEM. Characteristics including core loss are compared with ones without PWM waveform according to reference speed.

Keywords: Blushless DC motor, Core loss, Pulse width modulation, Switching frequency.

1. Introduction

Nowadays, it is important to analyze the losses such as core loss, copper loss and stray load loss in order to assess exact efficiency on the design stage of the motor. These losses are the main sources of heat generation. For the compact design and low operating cost of the system, these should be decreased when designing motor. Especially, core loss is increased remarkably at high speed. A lot of studies on the core loss of motor have been conducted by engineers [1-4]. However, these are based on ideal input voltage or current without inverter switching. In case of inverter driven motor, input voltage to the motor has harmonics due to switch pattern of inverter for pulse width modulation (PWM). The voltage with PWM waveform makes the current with harmonics. Therefore, core loss as well as copper loss is remarkably increased due to magnetic flux fluctuation in the core by current harmonics [5, 7]. Therefore, the analysis methodology for core loss considering PWM switching pattern of inverter is necessary in order for the exact assessment of system efficiency. K. Yamazaki researched analysis method for eddy current loss in the permanent magnets of motor by inputting ideal PWM waveform to FEM model [8]. However, it is difficult to consider the PWM voltage waveform due to control algorithm and carrier frequency.

The speed of blushless DC (BLDC) motor is generally controlled by PWM by changing duty ratio of switch at certain carrier frequency. In case of inverter driven motor such as BLDC, its efficiency is vary depending on carrier frequency, duty ratio, reactance of motor, etc. Therefore, loss analysis considering inverter parameters is necessary.

In this paper, inverter model including duty ratio control strategy is introduced in order to make PWM voltage waveform and BLDC motor model with equivalent circuit is used for the calculation of current waveform with harmonics from the PWM voltage waveform. Next, the characteristics of BLDC motor are analyzed by using FEM in which current waveform is a source of magneto-motive force. And then the core loss by proposed method is compared with that by ideal current waveform without PWM switching strategy. Finally the core loss is also compared with experimental one.

† Corresponding Author: Department of Electrical Engineering, Hanbat National University, Korea. (kckim@hanbat.ac.kr)
Received : July 20, 2014; Accepted : September 14, 2014

2. Analysis Model of Inverter Driven BDLC Motor

The application of the inverter driven BLDC motor introduced in the paper is for electric compressor. Fig. 1 shows the analysis model of BLDC motor. It has 6 poles and 9 slots combination. For the compact design, it is wound with concentrated winding. The material of permanent magnet is ferrite. The inverter makes controllable voltage for speed reference by using duty ratio parameter. Table 1 shows the brief specification of BLDC motor and inverter for the analysis.

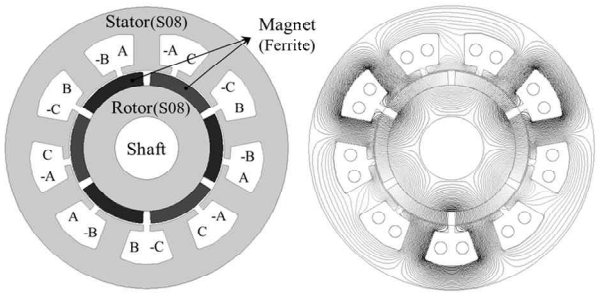

Fig. 1. Analysis model of BDLC motor

Table 1. Specification of the BLDC motor and inverter

Parameter			Specification	Unit
Motor	Power		27	W
	Torque		172	mNm
	Base-Speed		1,500	rpm
	Phase	R	5.76	ohm
		L_{self}	28.64	mH
		L_{mutual}	12.80	mH
		$L_{end\ leakage}$	1.10	mH
Inverter	Switching Frequency		5	kHz
	Battery Voltage		300	Vdc
	Duty Ratio		0.398	base

3. Co-simulation Model of Inverter Driven BLDCM

For the exact loss analysis, the co-simulation model for inverter driven BLDC motor including PWM switching algorithm based on ANSYS Simplorer software is introduced as shown in Fig. 2. The co-simulation model has inverter with 6 MOSFET switches which can be turn on and off by PWM sub-controller and BLDC motor model with equivalent circuit. Each of switching devices has 120° electric conduction region in which PWM with duty ratio is applied. For the simplicity of analysis, dead time of them against arm short is not considered in the model.

3.1 Analysis model of BLDC motor

The equivalent circuit is configured based on the voltage equation of the BLDC motor as shown in (1)

$$\begin{aligned} v_a &= R_s i_a + (L_s - M + L_{end})\frac{di_a}{dt} + E_a \\ v_b &= R_s i_b + (L_s - M + L_{end})\frac{di_b}{dt} + E_b \\ v_c &= R_s i_c + (L_s - M + L_{end})\frac{di_c}{dt} + E_c \end{aligned} \quad (1)$$

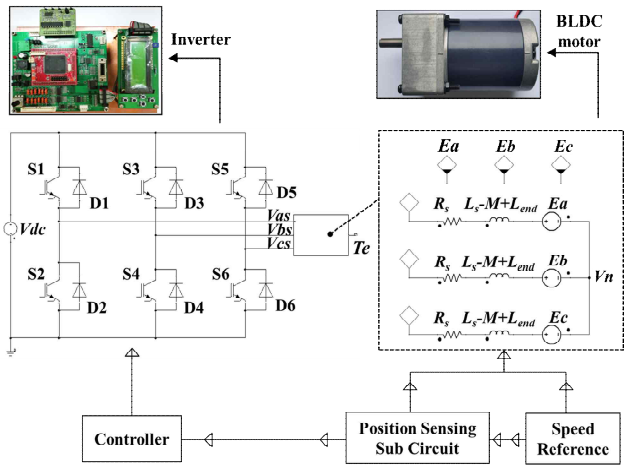

Fig. 2. Co-simulation model of inverter driven BLDC motor

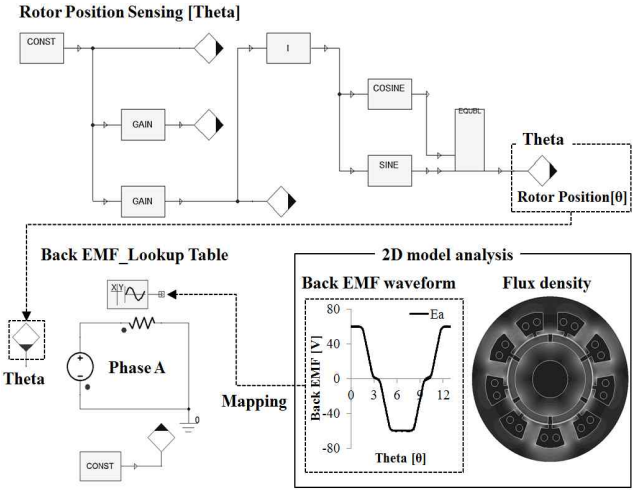

Fig. 3. Position sensing sub-circuit of the simulation model

where v_a, v_b, v_c are phase voltages; R_s is winding resistance; i_a, i_b, i_c are phase currents of each stator winding; E_a, E_b, E_c are phase back EMFs; L_s is self-inductance; M is mutual-inductance; L_{end} is leakage-inductance of end winding.

In the simulation model in Fig. 2, the back EMF E_a, E_b, E_c generated by 2D FEM of BLDC motor is directly used as lookup table. Because equivalent circuit parameters are derived from 2D FEM, the leakage inductance of end winding should be included in the model.

For the calculation of output torque, T_e for the feedback control, output power, P_e is divided by angular velocity of rotor, ω_m as shown in (2) and (3).

$$P_e = E_a i_a + E_b i_b + E_c i_c \quad (2)$$

$$T_e = \frac{P_e}{\omega_m} = \frac{1}{\omega_m}(E_a i_a + E_b i_b + E_c i_c) \quad (3)$$

Fig. 3 shows the position sensing sub-circuit of the simulation model in order to determine rotor position. When speed reference of controller is given, the rotor position angle is calculated as theta through the position sensing sub-circuit. The parameter of rotor position angle is used for two parts in the co-simulation model. First, theta is needed to select back EMFs from the lookup table in the equivalent circuit of BLDC motor. Second, it is needed to decide the switching sequence of the inverter in the controller sub-circuit.

3.2 Analysis model of inverter considering PWM control

For the exact loss assessment, inverter model considering PWM voltage waveform should be adopted in the co-simulation model. In the paper, in order to make control voltage from battery voltage, duty ratio technique is used.

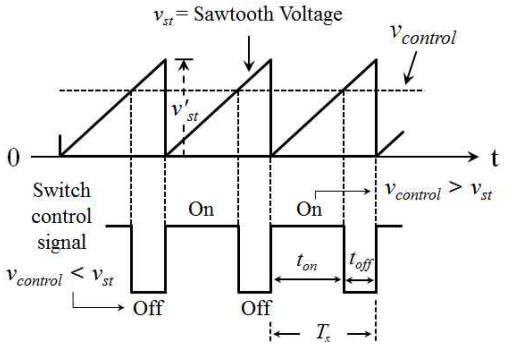

Fig. 4. PWM duty ratio control technique of BLDC motor

As shown in Fig. 4, On and Off states of switch control signal are determined through the comparison between saw tooth voltage, v_{st} with a certain carrier frequency and control voltage, $v_{control}$. When the control voltage is greater than the saw tooth voltage, the switch is 'Turn On'. Inverse case, it is 'Turn Off'.

The interval time of 'Turn On' and 'Turn Off' could be changed by the ratio of the amplitude of the saw tooth voltage, v'_{st} and control voltage, $v_{control}$. T_s is sum of the switch On and Off time. The switching frequency is also represented by the reciprocal of the cycle in (4). The switching duty ratio, D is the ratio of turn on time, t_{on} and T_s in (5)

$$f_s = \frac{1}{T_s} \tag{4}$$

$$D = \frac{t_{on}}{T_s} = \frac{v_{control}}{v'_{st}} \tag{5}$$

Conditional block of state equation for determining the switching operation as shown in Fig. 6 is represented by

$$\begin{aligned} &Switch\ Turn\ On\ :\ v_{control} > v_{st} \\ &Switch\ Turn\ Off\ :\ v_{control} < v_{st} \end{aligned} \tag{6}$$

The PWM technique is classified as the bipolar and unipolar switching patterns according to the conduction and switching patterns as shown in Fig. 5. In case of unipolar switching pattern, it can reduce switching loss. It also has the advantage of a smaller current ripple. For this reason, unipolar switching pattern is usually used to control the BLDC motor. In the paper, unipolar H_PWM-L_ON pattern in Fig. 5 (c) is used to make PWM voltage waveforms for the loss analysis of inverter driven BLDC motor. Next, it is compared with the result of ideal case without switching pattern in order to verify the loss difference due to PWM voltage waveforms.

Fig. 6 shows control sub-circuit for PWM voltage waveforms based on duty ratio in the co-simulation model. The state of 6 MOSFET switch control signal can be decided through comparison between saw tooth voltage, v_{st} and control voltage, $v_{control}$ due to duty ratio. Reference

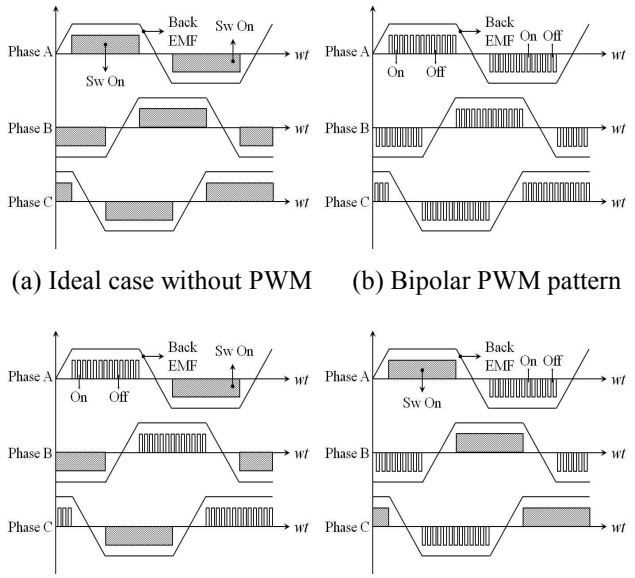

(a) Ideal case without PWM (b) Bipolar PWM pattern

(c) Unipolar H_PWM-L_ON (d) Unipolar H_ON-L_PWM

Fig. 5. Switching patterns of PWM in the inverter

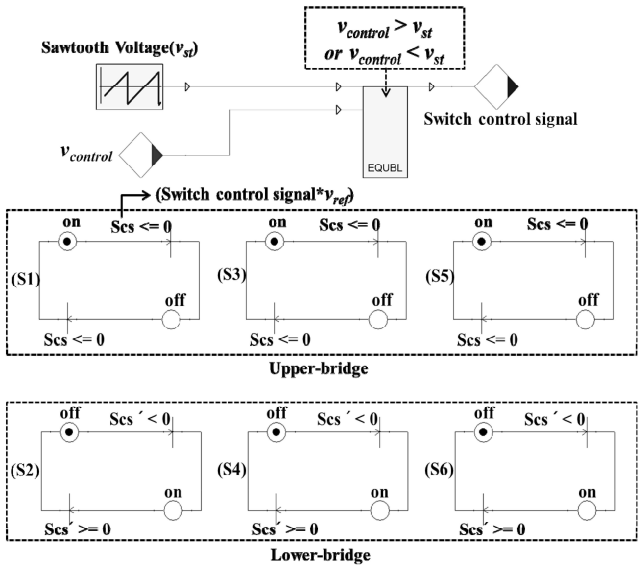

Fig. 6. PWM Control sub-circuit in the co-simulation

voltage, v_{ref} has a 120° flatted waveform with amplitude of 1 as shown in Fig. 5 (a). Multiplying these two parameters of the switch control signal and reference voltage, v_{ref}, the final PWM output signal can be generated.

3.3 The comparison of current and voltage waveforms between simulation and experiment

Through the co-simulation model for inverter driven BLDC motor in Fig. 2, the current and voltage waveforms can be extracted in Figs. 7 (a) and (c). The simulation results are similar to experiment results with proto-type having same carrier frequency and PWM duty ratio.

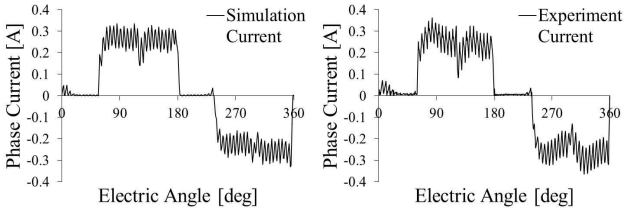

(a) Simulation current (b) Experiment current

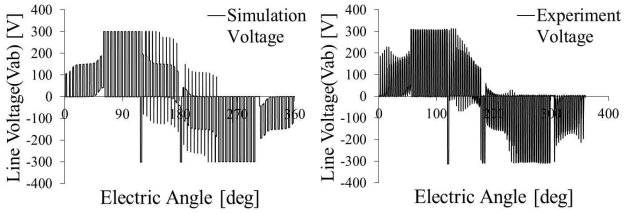

(c) Simulation voltage (d) Experiment voltage

Fig. 7. Current and voltage waveforms between the simulation and the experiment

4. Comparison Results on Core Loss

4.1 Comparison according to switching patterns

Figs. 8 and Fig. 9 show analysis results by inputting current waveforms generated from co-simulation model to 2D FEM as a current source. The analysis results in Fig. 8 are derived from ideal switch pattern of inverter without PWM control. On the other hand, the results in Fig. 9 show the waveforms with harmonics because of unipolar H_PWM-L_ON switch pattern.

Fig. 10 shows harmonics on phase current by FFT analysis.

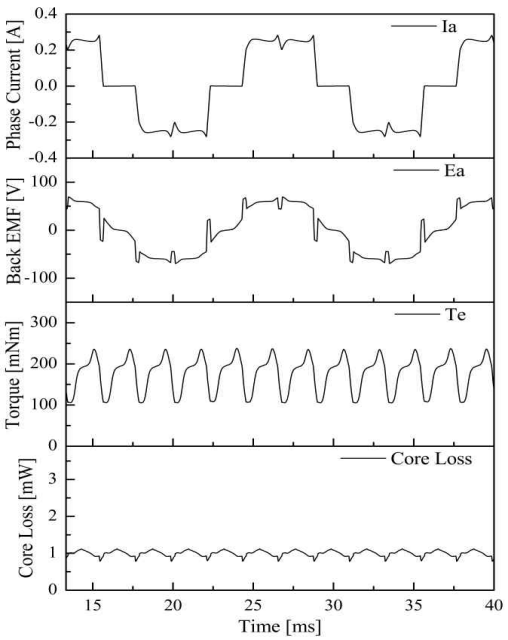

Fig. 8. Analysis results of ideal pattern (@1,500rpm)

As a result of FFT analysis of phase current with ideal switch pattern, harmonics over 45th nearly does not included. However, in case of PWM switch pattern, there are harmonics over 60th harmonics due to carrier frequency for duty ratio control.

The harmonics on PWM voltage waveform by duty ratio control based on carrier frequency generate current ripple and affects the ripple of back EMF waveform. The torque

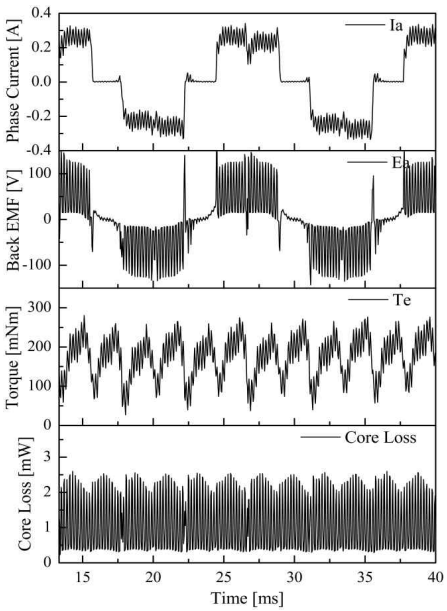

Fig. 9. Analysis results of PWM pattern (@1,500rpm)

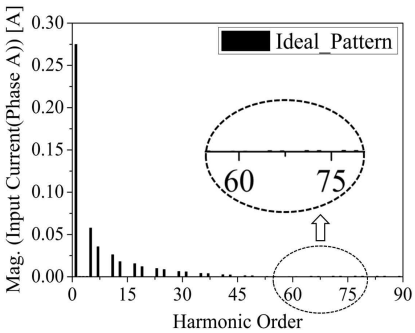

(a) Ideal pattern

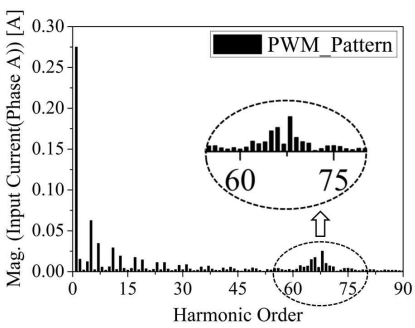

(b) PWM pattern

Fig. 10. Harmonics of phase current according to switching patterns (@1,500rpm)

of BLDC motor is occurred by multiplying the current and the back EMF. Therefore, the torque ripple is increased due to harmonics. In addition, the core loss between ideal and PWM switching patterns show distinct difference in the waveform. The core loss density by current harmonics is increased remarkably.

For the analysis of coreloss including harmonic effect, ANSYS Maxwell software is used by inputting several magnetic flux density vs. coreloss curves according to frequencies from 30 Hz to 2,000 Hz as shown in Fig. 11.

Fig. 12 shows the core loss distributions in the core of BLDC motor according to PWM switch patterns. The inside region of dotted line indicates region having core loss over 30kW/m^3. Due to the current harmonics by PWM switch pattern, the region of core loss is also expanded.

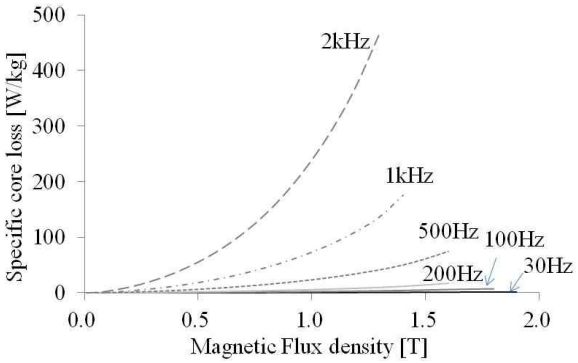

Fig. 11. B-P curves for the finite element analysis

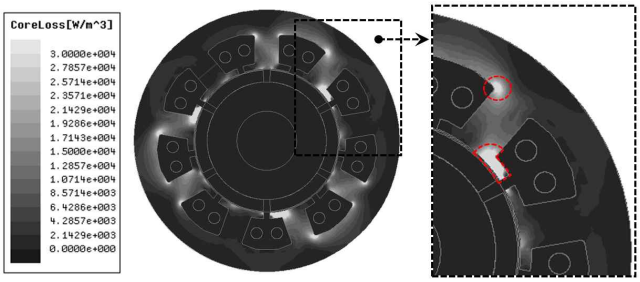

(a) Ideal Switch Pattern

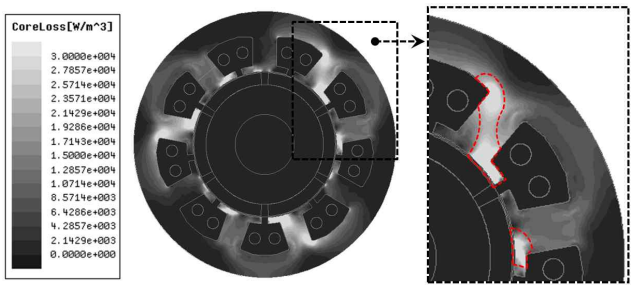

(b) PWM Switch Pattern

Fig. 12. Core loss distribution according to switching patterns (@1,500rpm)

4.2 Comparison according to motor speed without changing carrier frequency

In general, core loss increases rapidly according to motor speed. However, harmonics of phase current are changed with motor speed due to fixed carrier frequency, it is necessary to analyze the core loss according to motor speed.

Fig. 13 shows the analysis results with current waveform

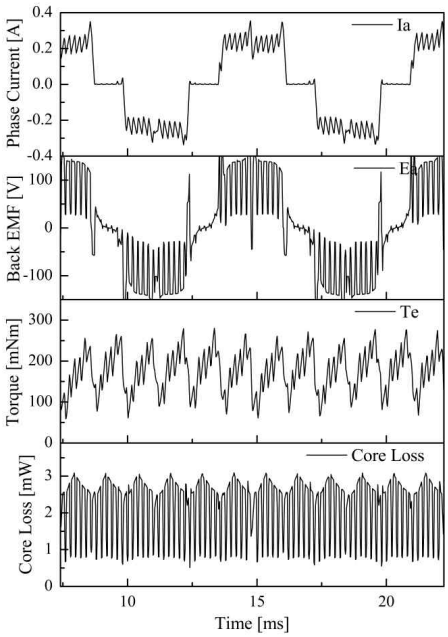

Fig. 13. Analysis results of PWM switch pattern (@2,700 rpm)

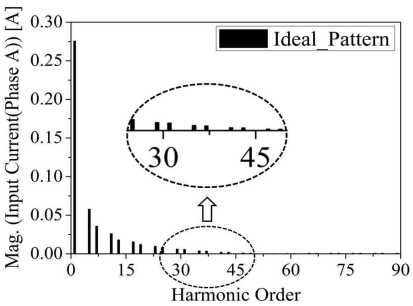

(a) Ideal pattern

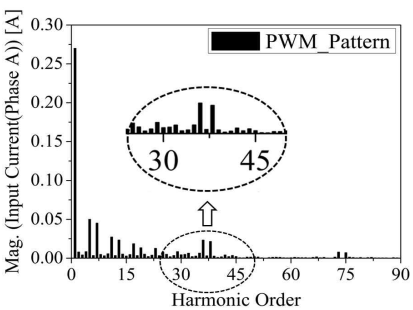

(b) PWM pattern

Fig. 14. Harmonics of phase current according to switching patterns (@2,700rpm)

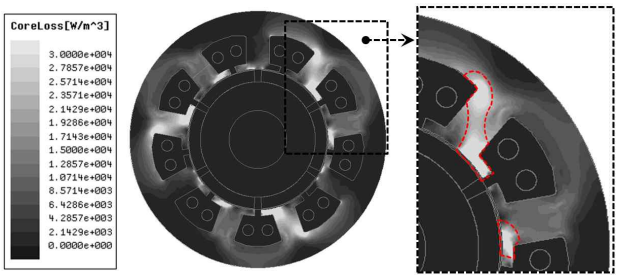

(a) 1500rpm

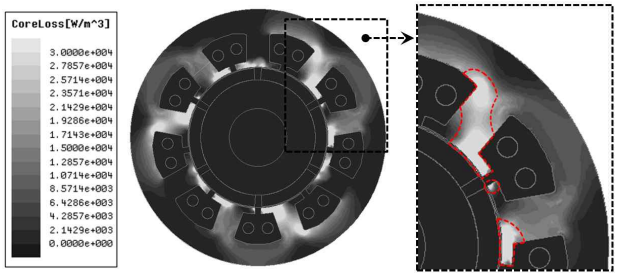

(b) 2700rpm

Fig. 15. Core loss distribution according to motor speed

of the PWM switch pattern at 2,700rpm. The carrier frequency of 5 kHz is same with 1,500rpm. In Fig. 14, phase current with ideal switch pattern almost does not include harmonics over 30th. On the other hand, in case of PWM switch pattern, there are harmonics above 30th harmonics due to carrier frequency. The harmonics is also varied according to motor speed. The region of core loss generation is expanded at high speed operation in Fig. 15.

Analysis results of total harmonic distortion (THD) on phase current according to PWM switching patterns are shown in Table 2. Although fundamental component of phase current is about 0.27A regardless of switch patterns, THD is different because of the harmonics by carrier frequency for PWM control. Finally, analysis results of inverter driven BLDC motor is showed in Table 3.

Because THD of current waveform by PWM is 7% larger than that of ideal switch pattern at 1,500rpm, the torque ripple of the analysis model with PWM control considering carrier frequency increases about 70%. Both iron loss and copper loss also increase about 119mW and 12.7mW respectively. For this reason, the efficiency is approximately decreased about 0.5%.

For the validity of the simulation results, coreloss is measured on the dynamometer by subtracting mechanical loss and copper loss out of total loss which can be derived

Table 2. THD results according to switching patterns

Switching pattern		THD [%]	Fundamental current [A]	Harmonic current [A]
1,500 rpm	Ideal	28.79	0.275	0.079
	PWM	35.98	0.275	0.099
2,700 rpm	Ideal	28.83	0.276	0.079
	PWM	34.04	0.270	0.092

Table 3. Characteristics of inverter driven BLDC motor

Parameter	Unit	Ideal	PWM	
Speed	[rpm]	1,500	1,500	2,700
Phase current	[Arms]	0.2025	0.2060	0.2011
Back EMF	[Vrms]	47.76	62.38	95.27
Torque	[mNm]	175.60	173.88	174.22
Torque ripple	[%]	75.57	145.65	127.04
Core loss	[mW]	996.8	1115.8	2141.8
Copper loss	[mW]	714.20	726.90	719.83
Efficiency	[%]	94.16	93.68	94.51

from input power and output power of BLDC motor. Coreloss is measured as 1,080 mW at 1,500 rpm and 2,020 mW at 2,700 rpm respectively.

In case of different carrier frequency at fixed rated operating point, the higher the carrier frequency is induced, the lower the coreloss is occurred.

5. Conclusion

The analysis method for the characteristics of inverter driven BLDC motor is proposed by using co-simulation model of inverter and motor in the paper. In general, ideal switch pattern of inverter is used at design stage of BLDC motor. However, it is difficult to assess core loss as well as copper loss due to harmonics of voltage and current. Especially characteristics of motor are affected by inverter parameters such as carrier frequency, duty ratio and frequency of voltage, etc. By using the proposed method, increase on core loss of inverter driven BLDC motor can be assessed qualitively rather than exact quantitive core loss and effective motor design can be realized considering these inverter parameters.

Acknowledgements

This research was supported by Basic Science Research Program through the National Research Foundation of Korea(NRF) funded by the Ministry of Science, ICT & Future Planning(2014R1A1A1006069)

References

[1] K.Y. Jung, Z. Ren, H.S. Yoon, C.-S. Koh, “Measurement of stator core loss of an induction motor at each manufacturing process,” *J. Electr. Eng. Technol.,* vol. 9, No. 4, pp. 1309-1314, 2014.

[2] K. Yamazaki, “Torque and efficiency calculation of an interior permanent magnet motor considering harmonic iron losses of both the stator and rotor,” *IEEE Trans. Magn*., vol. 39, no. 3, pp. 1460-1463, May 2003.

[3] Y. Huang, J. Dong, J. G. Zhu, Y. Guo, “Core loss

modeling for permanent magnet motor based on flux variation locus and finite element method," *IEEE Trans. Magn*., vol. 48, no. 2, pp. 1023-1026, Feb. 2012.

[4] N. Kunihiro, T. Todaka, M. Enokizono, "Loss evaluation of an induction motor model coreby vector magnetic characteristic analysis," *IEEE Trans. Magn*., vol. 47, no. 5, pp. 1098-1101, May. 2011.

[5] Jian Shi and Tie-Cai Li, "New Method to Eliminate Commutation Torque Ripple of Brushless DC Motor With Minimum Commutation Time, " *IEEE Trans.on Indus. Electron.*, Vol. 60, no. 6, pp. 2139-2146, June 2013.

[6] H. Domeki, Y. Ishihara, C. Kaido, Y. Kawase, S. Kitamura, T. Shimomura, N. Takahashi, T. Yamada, and K. Yamazaki, "Investigation of benchmark model for estimating iron loss in rotating machine," *IEEE Trans. Magn*., vol. 40, no. 2, pp. 794-797, Mar. 2004.

[7] K. Atallah, Z. Q. Zhu, and D. Howe, "An Improved method for predicting iron losses in brushless permanent magnet motor," *IEEE Trans. Magn*., vol. 28, no. 5, pp. 2997–2999, Sept. 1992.

[8] K. Yamazaki, S. Watarim, "Loss analysis of permanent-magnet motor considering carrier harmonics of PWM inverter using combination of 2-D and 3-D Finite-Element Method," *IEEE Trans. on Magn*., vol. 41, No. 5, pp. 1980-1983, May. 2005.

Ki-Chan Kim was born in Korea on August 8, 1972. He received his B.S., M.S., and Ph.D. degrees in Electrical Engineering from Hanyang University, Seoul, Korea in 1996, 1998 and 2005, respectively. He worked for Hyundai Heavy Industries Co., Ltd. from 1998 to 2005. Currently, he is an Assistant Professor in Electrical Engineering at Hanbat National University, Daejeon, Korea. His special area of interest includes the design and analysis of electrical motor and sensors.